JOURNAL OF CATALYSIS **161,** 651–658 (1996)
ARTICLE NO. 0227

Titania–Silica Mixed Oxides

IV. Influence of Ti Content and Aging on Structural and Catalytic Properties of Aerogels

D. C. M. Dutoit, M. Schneider,[1] R. Hutter, and A. Baiker[2]

Department of Chemical Engineering and Industrial Chemistry, Swiss Federal Institute of Technology, ETH-Zentrum, CH-8092 Zürich, Switzerland

Received October 12, 1995; revised March 5, 1996; accepted March 6, 1996

Titania–silica mixed oxide aerogels semicontinuously extracted with supercritical CO_2 have been shown to be promising catalysts for the epoxidation reaction of various bulky reactants. In this study, the amount of titania in the silica matrix and the aging time of the wet sol–gel product were varied in order to optimize the structural and chemical properties of this material for the use as epoxidation catalysts. Additional preparation parameters involved are the prehydrolysis of the silicon alkoxide and the amount of acid added during the wet sol–gel step. The samples were characterized by means of nitrogen physisorption, elemental analysis, FTIR, Raman and UV–Vis spectroscopies, and XRD. The catalytic activity was tested using cyclohexene and α-isophorone epoxidation. The highest contribution of Si–O–Ti entities, as derived from FTIR measurements, was found for samples with 30 wt% nominal TiO_2, whereas the optimum Ti-dispersion is achieved with a content of 20 wt% TiO_2. Optimum textural properties were obtained after aging the sol–gel batch for 240 h before the supercritical CO_2 extraction procedure. Reducing the amount of acid in the hydrolysant lowered the catalytic activity. The optimum aerogel preparation parameters derived from this study are 20 wt% nominal TiO_2, an aging period of 240 h, at least an acid amount with a molar ratio water : alkoxide : acid of 5 : 1 : 0.09, and no prehydrolysis.

INTRODUCTION

In parts I–III (1–3) of this work titania–silica mixed oxides were prepared, characterized, and tested in epoxidation reactions of different bulky reactants. Selectivities and initial rates were generally higher with the low-temperature aerogels compared to TiO_2 on SiO_2-systems, zeolites, high-temperature aerogels, and conventionally dried xerogels. The catalytic activity resided in advantageous structural properties, i.e., mesoporosity and high Ti-dispersion determined by FTIR analysis of the catalysts. An increase of the Ti-content from 2 to 20 wt% TiO_2 led to a concomitant rise in Si–O–Ti heteroconnectivity and initial rate of epoxidation. These findings indicated that there must be an optimum Ti/Si ratio for maximizing the amount of Si–O–Ti connectivities. Furthermore the Ti/Si ratio was found to influence the textural properties and thereby the accessibility of the active Ti sites for the reactants.

Another potent means of controlling the textural properties is the aging procedure (4–9). Rangarajan *et al.* (8) showed that aging alcogels in their pore liquid resulted in reduced drying shrinkage. Scherer (9) claimed that aging may cause coarsening of pores and loss of surface area if the solubility of the solid phase is high enough. The formation of new cross-links produces shrinkage (syneresis) and increases the modulus and viscosity of the gel, so that aging reduces the subsequent shrinkage during drying.

The difficulties in producing intimately mixed oxides are discussed in part I (1). The solution–sol–gel (SSG) technique represents a highly controllable preparation route (4, 10) with inherent advantages such as molecular-scale mixing of the constituents, purity of the precursors, homogeneity of the sol–gel product (prominent isotropy), and the use of different wet-chemical preparation tailoring tools such as the molar ratios water : alkoxide : acid and prehydrolysis of the less reactive silicon alkoxide. Concentration of hydrolysant (water) and catalyst (hydrochloric acid) determine the resulting hydrolysis and condensation conditions of the applied silicon and modified titanium alkoxides (10, 11). The acidic medium stabilizes the TiOH and SiOH groups against ensuing homo condensation reactions (1 and references therein). However, Handy *et al.* (12) found that acid catalysis in combination with prehydrolysis resulted in formation of a very weak wet-gel structure.

As to prehydrolysis, we showed in part I (1) that at Ti contents of $\leq$10 wt% nominal TiO_2, the BET surface area declined and the microporosity increased at the preparation conditions chosen. At 20 wt% nominal TiO_2, the influence on the textural properties determined by nitrogen physisorption was very small. The estimate of Ti-dispersion by FTIR indicated no significant influence of the prehydrolysis procedure. Miller *et al.* (13) could improve the mixing efficiency in titania–silica aerogels with prehydrolysis

[1] Present address: F. Hoffmann-La Roche Ltd., VFH, CH-4070 Basel, Switzerland.

[2] To whom correspondence should be addressed.

0021-9517/96 $18.00

as indicated by 1-butene isomerization activity tests. The different behavior can be explained by the use of different Ti precursors; in part I (1) we employed chemically modified tetraisopropoxytitanium (IV) and Miller *et al.* (13) used unmodified tetrabutoxytitanium (IV). Therefore we compensated for the different alkoxide reactivities of silicon and titanium by mainly chemical modification along with prehydrolysis, whereas Miller *et al.* used prehydrolysis alone.

In the present work, we have extended the Ti-content of the aerogels from 20 to 70 wt% nominal TiO_2 in SiO_2 and studied its influence on the structural properties and the catalytic behavior in the epoxidation of cyclohexene and α-isophorone. In addition, effects of prehydrolysis, amount of hydrolysant (HCl), and aging time were investigated.

METHODS

Preparation Procedures

The set of acronyms used in this work is built up as follows: The first numeral displays the nominal TiO_2 content in wt%, based on the theoretical system TiO_2–SiO_2 (20 wt% "TiO_2" → 15.8 at.% Ti; 30 wt% → 24.3 at.%; 50 wt% → 42.9 at.%; 70 wt% → 63.6 at.%); the subsequent two capital letters "*LT*" stand for low-temperature supercritically dried; "s" stands for molar ratios H_2O : alkoxide : acid of 5 : 1 : 0.045 instead of 5 : 1 : 0.09 as used in all other samples; "p" indicates prehydrolysis [the prehydrolysis procedure is described in (1)]; the last numeral displays the aging period of the wet sol–gel product before the extraction procedure in hours, 6.5m means aged over 6.5 months.

The wet-chemical preparation procedure used and the findings concerning sol–gel reactivities are described in detail in Ref. (1). In brief, tetraisopropoxytitanium (IV) (TIPOT; Fluka, pract.) was chemically modified with acetylacetone (acac; Fluka, puriss., p.a.). Modified TIPOT and tetramethoxysilicon (IV) (TMOS; Fluka, puriss., p.a.) were dissolved in i-PrOH. The hydrolysant added consisted of doubly distilled water and hydrochloric acid (HCl 37 wt%; Fluka, puriss., p.a.). Quantities and aging periods of the appropriate sol–gel samples are listed in Table 1. The total volume of the SSG sample was ca. 200 ml and the corresponding molar ratios of doubly distilled H_2O : alkoxide : hydrochloric acid were 5 : 1 : 0.09 and 5 : 1 : 0.045 in the samples 20*LT*s720 and 20*LT*ps6.5m.

Semicontinuous extraction with supercritical carbon dioxide was performed with all samples resulting in low-temperature aerogels. At a temperature of 313 K, the autoclave with a net volume of 2 dm^3 was pressurized with supercritical CO_2 to 24 MPa and the liquid–gas separator to 1 MPa, which resulted in an overall amount of 2.3 kg CO_2. The solvent of the SSG product was semicontinuously extracted by a CO_2 flow of 20 g min^{-1} for 5 h (6 kg CO_2) at a temperature of 313 K. The pressure was then isothermally released at ca. 20 g min^{-1}. Finally, the system was allowed to cool to ambient temperature. Prior to characterization and catalytic tests the resulting aerogel clumps were carefully ground in a mortar to powder.

TABLE 1

Quantities, Compositions, and Aging Times of the Sol–Gel Preparations

Sample	TIPOT (mod.)[a] (mmol)	TMOS[b] (mmol)	HCl, 37 wt% (mmol)	H_2O (mmol)	i-PrOH (mol)	Aging time[c] (h)
20*LT*48	28	150	16.0	889	1.6	48
20*LT*240	28	150	16.0	889	1.6	240
20*LT*720	28	150	16.0	889	1.6	720
20*LT*s720	28	150	8.0	889	1.6	720
20*LT*ps6.5m	28	150	8.0	889	1.6	4600
30*LT*720	45	140	16.7	925	1.6	720
50*LT*720	75	100	15.7	875	1.6	720
70*LT*720	105	60	14.9	825	1.6	720

Note. Designations of the samples are explained under Methods.

[a] Tetraisopropoxytitanium (IV) complexed with acetylacetonate [TIPOT(mod.)].

[b] Tetramethoxysilicon (IV) (TMOS).

[c] Aging at ambient temperature, without stirring, hermetically closed, under nitrogen, no light.

Portions of the uncalcined (raw) aerogel powder were calcined in a tubular reactor with upward flow. The temperature given corresponded to the oven temperature. The sample amount was ca. 2 g in all cases. To remove most of the organic residues prior to calcination in air, all aerogel samples were first heated at 5 K min^{-1} to 673 K in a nitrogen flow of 0.5 dm^3 min^{-1} and then kept under these conditions for 1 h. Subsequently the samples were cooled to ca. 353 K, and heated again at 5 K min^{-1} in air flowing at 0.5 dm^3 min^{-1} and then kept for 5 h at 673 or 873 K under these conditions.

The composition was generally calculated on the basis of the nominal amounts used (Table 1) and independently confirmed by inductively coupled plasma atomic emission spectroscopy (ICPAES).

Physico-chemical Characterization

The characterization procedures are described in more detail in Refs. (1, 2).

Nitrogen physisorption. The specific surface areas (S_{BET}), mean cylindrical pore diameters ($\langle d_p \rangle$), and specific desorption pore volumes ($V_{p(N_2)}$) were determined by nitrogen physisorption at 77 K using a Micromeritics ASAP 2000 instrument. $V_{p(N_2)}$ was assessed by the Barrett–Joyner–Halenda (BJH) method (14), which is assumed to cover the cumulative desorption pore volume of pores in the maximum range 1.7–300 nm diameter. S_t and V_t denote specific micropore surface area and pore volume, respectively,

derived from *t*-plot analysis in the range $0.3 < t < 0.5$ nm, using the Harkins–Jura correlation (15).

X-ray diffraction. X-ray powder diffraction (XRD) patterns were measured on a Siemens Θ/Θ D5000 powder X-ray diffractometer using Cu$K\alpha$ radiation.

FTIR spectroscopy. FTIR measurements were performed on a Perkin Elmer Series 2000 instrument. Sample wafers consisted of 100 mg dry KBr and ca. 1 mg sample. The sample cell was purged with a small flow of oxygen during the measurements. Five hundred scans were accumulated for each spectrum in transmission, at a spectral resolution of 4 cm^{-1}. The spectrum of dry KBr was taken for background subtraction. The FTIR-spectra of titania–silica mixed oxides are characterized by a typical band at 940–960 cm^{-1}, assigned to framework titanium which is usually quoted for the semiquantitative estimate of the Si–O–Ti connectivity (1). For the evaluation of the FTIR results four bands were deconvoluted into Gaussian curves. The estimate of Si–O–Ti connectivity (Ti dispersion), $D_{(Si–O–Ti)}$, is defined in Eq. [1]:

$$D_{(Si–O–Ti)} = \frac{S_{(Si–O–Ti)}}{S_{(Si–O–Si)}} \cdot \frac{x_{Si}}{x_{Ti}}. \qquad [1]$$

$S_{(Si–O–Ti)}$ and $S_{(Si–O–Si)}$ are the deconvoluted peak areas of the ν(Si–O–Ti) band at ca. 940 cm^{-1} and the ν(Si–O–Si) band at ca. 1210 cm^{-1}, respectively; x_{Si} and x_{Ti} designate the molar proportions of Si and Ti, respectively. It is noteworthy to mention that a similar tendency of $D_{(Si–O–Ti)}$ was found if ν(Si–O–Si) at 800 cm^{-1} was used instead of the band at 1210 cm^{-1} in the definition; such $D_{(Si–O–Ti)}$-values are supposed to represent a semiquantitative measure of the proportion of Si–O–Ti species referred to the total Ti content and thus a kind of mixing efficiency or estimate of Ti dispersion.

FTRaman spectroscopy. For the Raman measurements the samples were transferred to 4 mm test tubes. Spectra were excited using the 1033 nm line of a YAG laser (Spectron Laser Systems). The back scattered light was analyzed by a Perkin Elmer Series 2000 instrument. The laser power used was 2W for the samples with a TiO_2 content ≤50 wt%, the thus-induced temperatures of the samples were ca. 720 K. For the sample containing 70 wt% TiO_2, 0.1 W was used. A total of 7000 scans were accumulated for each spectrum, at a spectral resolution of 2 cm^{-1}.

Thermal analysis. Total carbon and hydrogen contents were determined with a LECO CHN-900 elemental microanalysis apparatus.

UV–Vis analysis. UV–Vis diffuse reflection spectra measurements under environmental conditions were performed on a Perkin Elmer Lambda 16 spectrophotometer equipped with a 76 mm integrating sphere using $BaSO_4$ as reference. The samples were pretreated over 1 h at 410 K and 125 mbar, sealed, and cooled down to room temperature. The reflection in percentage was measured and presented by the Kubelka–Munk function.

Epoxidation reaction. The epoxidation procedures are described in detail in Refs. (2, 3). In brief, 16.7 ml (13.4 mmol) of 12 wt% cumene hydroperoxide (CHP) in cumene was charged in the dropping funnel. One hundred milligram catalyst and 7.8 ml (77 mmol) cyclohexene were introduced into the reactor. The solutions were heated to reaction temperature (333 K), and the reaction was started by adding the peroxide to the vigorously stirred slurry. The reaction rate (r_c) was defined as the epoxide formation in the first 300 s. The epoxidation of α-isophorone was carried out at 333 K with 200 mg catalyst, 77 mmol olefin, 13.4 mmol *t*-butylhydroperoxide (TBHP) in toluene, and 9 ml ethylbenzene as solvent. The reaction rate (r_α) is defined as the epoxide formation in the first 20 min.

RESULTS

Nitrogen Physisorption

Structural properties of the aerogels, raw and calcined in air at different temperatures, are listed in Tables 2 and 3. In general, the aerogels with a titania content of ≤30 wt% showed a type-IV isotherm with a type-H1 desorption hysteresis according to IUPAC classification (16) and mesoporosity with graphically determined maxima of the pore size distribution in the range 40–70 nm. After calcination in air at 673 K, the aerogels with Ti contents of ≤30 wt% nominal TiO_2 possessed BET surface areas in the range 674–811 $m^2\,g^{-1}$ (Tables 2 and 3). The samples 50*LT*720 and 70*LT*720 exhibited distinctly lower BET surface areas than the aerogels with less TiO_2 in the silica matrix (Table 2).

The influence of the aging period of the wet sol–gel product before the extraction procedure is shown in Fig. 1 and Table 3. An increase in aging time from 48 to 720 h led to a slight rise in BET surface area and microporosity for the samples calcined in air at 673 or 873 K. The specific nitrogen pore volume reached a maximum for the sample 20*LT*240 (Fig. 1). For investigating the influence of the acid quantity, the molar ratio water : alkoxide : acid was changed from 5 : 1 : 0.09 to 5 : 1 : 0.045 in the case of aerogel 20*LT*720, which possessed well-developed textural properties, resulting in aerogel 20*LT*s720. The corresponding samples calcined at 673 K did not exhibit significant differences. However, after calcination at 873 K, the appropriate sample of 20*LT*s720 possessed higher BET surface area and a distinctly higher specific pore volume. In essence, aging time and lower acid content had a positive influence on the textural properties of the aerogel, the latter especially at elevated temperatures. Sample 20*LT*ps6.5m was prepared using the molar ratio water : alkoxide : acid of 5 : 1 : 0.045, an aging period of 6.5 months, and the prehydrolysis procedure (1). The surface area of the sample calcined in air at 673 K amounted to 811 $m^2\,g^{-1}$ and the specific pore volume was 2.6 $cm^3\,g^{-1}$.

TABLE 2

Structural and Chemical Properties of the Aerogels Both Raw and Calcined in Air at Different Temperatures

Sample	Calc. (K)	S_{BET} (S_t)[a] (m^2/g)	$V_{p(N_2)}$ (V_t)[b] (cm^3/g)	$\langle d_p \rangle$[c] (nm)	$S_{(Si-O-Ti)}/S_{(Si-O-Si)}$[d]	$D_{(Si-O-Ti)}$[e]	C content[f] (%)
20*LT*720	—	642 (27)	3.04 (0.01)	18.9 (70)			13.1
	673	710 (168)	2.37 (0.07)	13.4 (60)			0.2
	873	617 (107)	2.57 (0.04)	16.7 (60)	0.72	3.8	0.1
30*LT*720	—	610 (60)	1.94 (0.00)	13 (70)			12.5
	673	741 (61)	2.48 (0.02)	13 (70)			0.9
	873	356 (42)	1.92 (0.00)	22 (60)	1.04	3.2	0.9
50*LT*720	—	329 (4)	1.77 (0.00)	22 (55)			15.9
	673	291(26)	1.62 (0.00)	22 (60)			1.5
	873	398 (18)	2.32 (0.00)	23 (70)	0.99	1.3	0.9
70*LT*720	—	142 (142)	0.006 (0.03)	0.2 (–)			29.2
	673	75 (36)	0.003 (0.02)	0.2 (–)			2.3
	873	16 (3)	0.004 (0.01)	1 (–)	0.44	0.3	1.1

Note. Designations of the samples are explained under Methods.

[a] (S_t) denotes specific micropore surface area derived from *t*-plot analysis.

[b] $V_{p(N_2)}$ designates the BJH cumulative desorption pore volume of pores in the maximum range 1.7–300 nm diameter. (V_t) denotes specific micropore pore volume derived from *t*-plot analysis.

[c] $\langle d_p \rangle = 4V_{p(N_2)}/S_{BET}$; in parentheses, the graphically assessed pore size maximum of the pore-size distribution derived from the desorption branch are given.

[d] Relative contribution of Si–O–Ti entities, estimated from the ratio of Si–O–Ti (ca. 940 cm^{-1}) and Si–O–Si (ca. 1210 cm^{-1}) peak areas.

[e] $D_{(Si-O-Ti)}$; estimate of Ti dispersion derived from Eq. [1].

[f] Total carbon contents determined by elemental microanalysis.

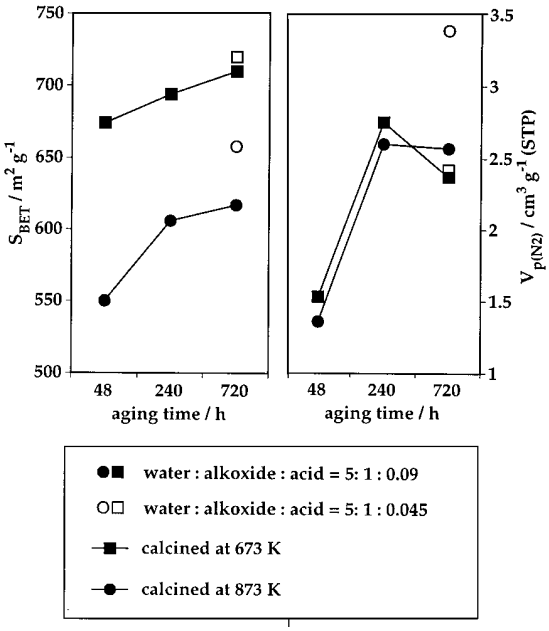

FIG. 1. Influence of the aging time of the wet sol-gel product before the extraction procedure and of the water : alkoxide : acid ratio on BET surface area and specific pore volume ($V_{p(N_2)}$) of the 20*LT* series, determined by nitrogen physisorption at 77 K (STP; 273.15 K, 1 atm). The samples were calcined in air at 673 or 873 K.

The graphically assessed pore size maximum of the pore-size distribution derived from the desorption branch was ca. 40 nm, which is lower than that of the samples 20*LT*240, 20*LT*720, 20*LT*s720, exhibiting corresponding values in the range 52–70 nm.

X-Ray Diffraction

X-ray analysis indicated that all low-temperature aerogels listed in Tables 2 and 3 were X-ray amorphous at temperatures ≤673 K. Only aerogel 70*LT*720 showed anatase crystallites after calcination in air at 873 K.

FTIR Spectroscopy

FTIR-spectra of the samples with different Ti contents calcined in air at 873 K are presented in Fig. 2. The band in the range 794–806 cm^{-1} indicates symmetric ν(Si–O–Si) stretching vibration (4, 17), 932–939 cm^{-1} ν(Si–O–Ti) vibration (18–20), 1081–1091 cm^{-1} asymmetric ν(Si–O–Si) stretching vibration (4, 17, 21), and 1196–1208 cm^{-1} asymmetric ν(Si–O–Si) stretching vibration (4, 17, 21). The band at ca. 940 cm^{-1}, indicative of Si–O–Ti species, is well-developed for the aerogels with up to 50 wt% TiO_2, but only weak for the aerogel 70*LT*720. This finding is in agreement with the results from X-ray analysis.

As an estimate for the abundancy of Si–O–Ti entities in the mixed oxide, the ratio of the deconvoluted peak areas ($S_{Si-O-Ti}/S_{Si-O-Si}$) and its normalized $D_{(Si-O-Ti)}$ value, defined in Eq. [1], were used (Table 2). The Si–O–Ti connectivity

TABLE 3

Structural Properties and C-Content of the 20 wt% TiO_2/80 wt% SiO_2 Aerogels Obtained with Different Preparation Conditions (Aging Time, Acid Addition, Prehydrolysis), Both Raw and Calcined in Air at Different Temperatures

Sample	Calc. (K)	S_{BET} (S_t)[a] (m^2/g)	$V_{p(N_2)}$(V_t)[b] (cm^3/g)	$\langle d_p \rangle$[c] (nm)	C content[d] (%)
20*LT*48	—	714 (82)	1.13 (0.03)	6.3 (40)	8.9
	673	674 (83)	1.53 (0.04)	9.1 (40)	4.5
	873	550 (32)	1.36 (0.01)	9.9 (40)	0.1
20*LT*240	—	426 (0)	3.05 (0.00)	28.6 (70)	11.3
	673	694 (127)	2.75 (0.05)	15.9 (60)	0.2
	873	606 (106)	2.60 (0.04)	17.2 (52)	0.1
20*LT*720	—	642 (27)	3.04 (0.01)	18.9 (70)	13.1
	673	710 (168)	2.37 (0.07)	13.4 (60)	0.2
	873	617 (107)	2.57 (0.04)	16.7 (60)	0.1
20*LT*s720	—	665 (16)	3.74 (0.00)	22.5 (60)	12.1
	673	720 (119)	2.38 (0.05)	13.2 (60)	0.2
	873	658 (67)	3.39 (0.02)	20.6 (62)	0.1
20*LT*ps6.5m	—	724 (76)	2.74 (0.03)	15.1 (43)	12.9
	673	811 (158)	2.60 (0.07)	12.8 (40)	0.7
	873	675 (101)	2.35 (0.04)	13.9 (40)	0.1

Note. Designations of the samples are explained under Methods.

[a] (S_t) denotes specific micropore surface area derived from *t*-plot analysis.

[b] $V_{p(N_2)}$ designates the BJH cumulative desorption pore volume of pores in the maximum range 1.7–300 nm diameter. (V_t), in parentheses, denotes specific micropore pore volume derived from *t*-plot analysis.

[c] $\langle d_p \rangle = 4V_{p(N_2)}/S_{BET}$; in parentheses, the graphically assessed pore size maximum of the pore-size distribution derived from the desorption branch are given.

[d] Total carbon contents determined by elemental microanalysis.

$D_{(Si–O–Ti)}$ is assumed to represent a relative measure of the proportion of Si–O–Ti species referred to the total Ti content and thus provides a kind of mixing efficiency, a quantity related to Ti dispersion [part I (1)]. The effect of the Ti content is displayed in Fig. 3 for the low-temperature aerogels nn*LT*720, all samples calcined in air at 873 K. An increase of the Ti content caused a distinct decrease of $D_{(Si–O–Ti)}$ (Fig. 3). Note, however, that the contribution of Si–O–Ti species expressed as $S_{(Si–O–Ti)}/S_{(Si–O–Si)}$ increased significantly up to 30 wt% TiO_2 and decreased at higher Ti content. Consequently, a maximum of Si–O–Ti species is contained in sample 30*LT*720. The 20*LT* samples listed in Table 3 revealed no significant differences in $S_{(Si–O–Ti)}/S_{(Si–O–Si)}$-values. The behavior suggests that in the range of conditions chosen aging time, acid amount, and prehydrolysis had no marked influence on the Ti dispersion estimated by FTIR analysis.

Raman Spectroscopy

The influence of the Ti content is also evident from the Raman spectra depicted in Fig. 4. Low-temperature aerogels 20*LT*720, 30*LT*720, and 50*LT*720, calcined in air at 873 K, show bands at 930 and 1100 cm^{-1}, which are both assigned to ν(Si–O–Ti) vibrations (4). The band at 1100 cm^{-1}, however, is superimposed by the asymmetric ν(Si–O–Si) stretching vibration at 1070 cm^{-1} (4). The band at 800 cm^{-1} is also found in pure silica xerogels (22).

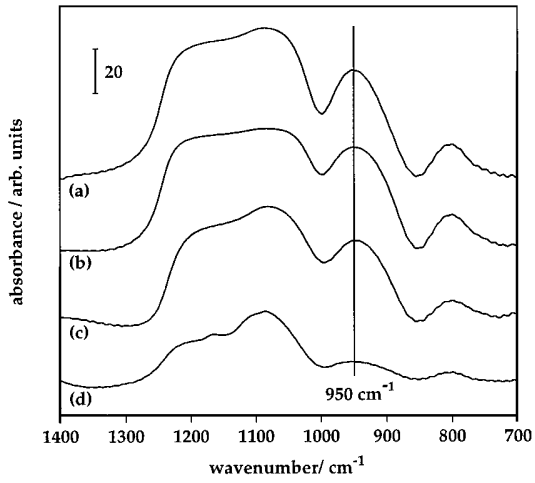

FIG. 2. FTIR spectra of titania–silica low-temperature (*LT*) aerogels with (a) 20 wt% (20*LT*720), (b) 30 wt% (30*LT*720), (c) 50 wt% (50*LT*720), and (d) 70 wt% nominal TiO_2 (70*LT*720); all samples were calcined in air at 873 K. Designations of samples are explained under Methods.

The very broad band at 430 cm^{-1} is assigned to Si–O–Si bending modes, and the band at ca. 480 cm^{-1} is attributed to defects in the network. Best and Condrate (23) assigned the broadening of the 430 cm^{-1} band with increasing Ti content in titania–silica systems to increasing incorporation of Ti into tetrahedral sites of the silica network with concomitant distortion of the SiO_4 tetrahedra (Fig. 4).

For the sample of aerogel 70*LT*720, calcined in air at 873 K, the presence of crystalline anatase emerges from the bands at about 380, 520, and 615 cm^{-1}, confirming the

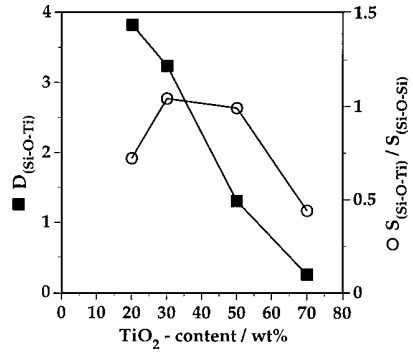

FIG. 3. Influence of the Ti content on the normalized Si–O–Ti connectivity ($D_{(Si–O–Ti)}$, defined in Eq. [1]) and on the contribution of Si–O–Ti species estimated from the ratio $S_{(Si–O–Ti)}/S_{(Si–O–Si)}$ (derived from FTIR measurements) of the low-temperature aerogels calcined in air at 873 K. $S_{(Si–O–Ti)}$ and $S_{(Si–O–Si)}$ represent the peak areas of the Si–O–Ti band at ca. 940 cm^{-1} and the Si–O–Si band at ca. 1210 cm^{-1}, respectively.

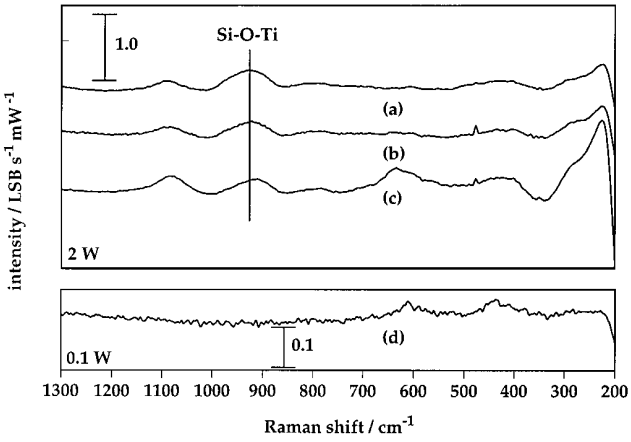

FIG. 4. Raman spectra of titania-silica *LT* aerogels with (a) 20 wt% (20*LT*720), (b) 30 wt% (30*LT*720), (c) 50 wt% (50*LT*720), and (d) 70 wt% nominal TiO_2 (70*LT*720); all samples are calcined in air at 873 K. Note that the laser power used for spectra (d) was 0.1 W, compared to 2 W used in the other spectra.

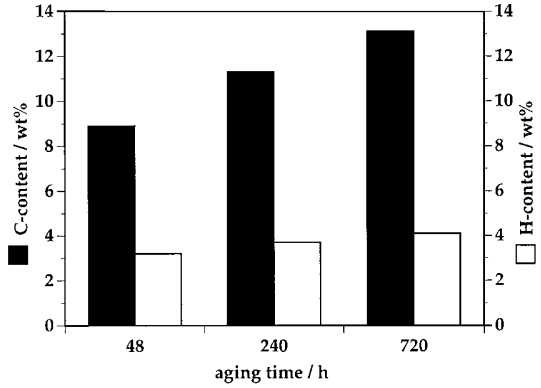

FIG. 5. Influence of the aging time of the wet sol–gel product before the extraction procedure on carbon and hydrogen content in the uncalcined aerogels of the 20*LT* series.

results of X-ray diffraction analysis. As to 50*LT*720, calcined at 873 K, the broad band at 635 cm^{-1} indicates some segregated anatase.

Thermal Analysis

All uncalcined aerogels contained remarkable amounts of carbon, as deduced from elemental microanalysis. The amount of elemental carbon increases with rising Ti content for samples containing ≥30 wt% nominal TiO_2 (Table 2). The uncalcined aerogel 70*LT*720 contains 29.2 wt% elemental C. These organic residues are likely to originate from the realkoxylation of surface hydroxyl groups and the incorporation of both unhydrolyzed alkoxide ligands and acetylacetonate, as well as residual solvent in the SSG matrix (24). The nn*LT*720-series shows an increase in the C content with longer aging times (Table 3, Fig. 5), whereas the hydrogen content remains virtually constant. It emerges from all calcination-series that the calcination at 673 K reduces the amount of organic contaminants drastically (Tables 2 and 3). Calcination in air at 873 K results in carbon contents of 0.1 wt% for the 20*LT* series, and ≤1.1 wt% for the nn*LT*720 series.

UV–Vis Analysis

UV–Vis spectroscopy is known to be a sensitive method for the characterization of titania–silica systems (2). Spectra of samples with different Ti contents are presented in Fig. 6. With a rise in Ti content of the titania–silica aerogels, the UV absorption edge shifts to lower wavenumbers. This shift in the spectra of the aerogel samples 20*LT*720, 30*LT*720, and 50*LT*720 indicates growing nanodomains of titania (1).

Epoxidation Reaction

In general, the uncalcined aerogels showed higher activities for epoxidation than the corresponding samples calcined in air at 673 or 873 K. The influence of the Ti content in titania–silica low-temperature aerogels on the catalytic activity is depicted in Fig. 7. Sample 10*LT* is included as a reference (2, 3). The initial rates for cyclohexene (r_c) and α-isophorone epoxidation (r_α) decrease at a Ti content higher than 20 wt% nominal TiO_2. For the epoxidation of cyclohexene, sample 20*LT*720 shows the highest rate ($r_c = 8.3$ mmol min^{-1} g_{cat}^{-1}) and aerogel 50*LT*20 the lowest rate ($r_c = 4.2$ mmol min^{-1} g_{cat}^{-1}). Sample 70*LT*720 was almost inactive. Calcination in air at 673 K led to lower catalytic activity (Fig. 7). The same tendencies were observed for the epoxidation of α-isophorone. Note, however, that r_α is about 45 times lower than r_c. This behavior is attributed to the electron-deficiency of the C=C double bond in isophorone which retards the epoxidation reaction.

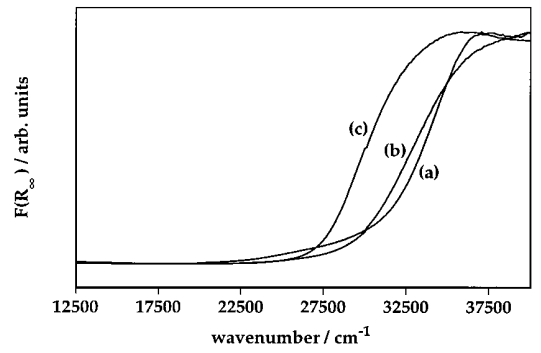

FIG. 6. Diffuse reflectance spectra of titania–silica *LT* aerogels with different titania contents. (a) 20 wt% (20*LT*720), (b) 30 wt% (30*LT*720), and (c) 50 wt% nominal TiO_2 (50*LT*720). All samples were calcined in air at 873 K. The samples were pretreated at 125 mbar and 410 K over 1 h. Designations of samples are explained under Methods.

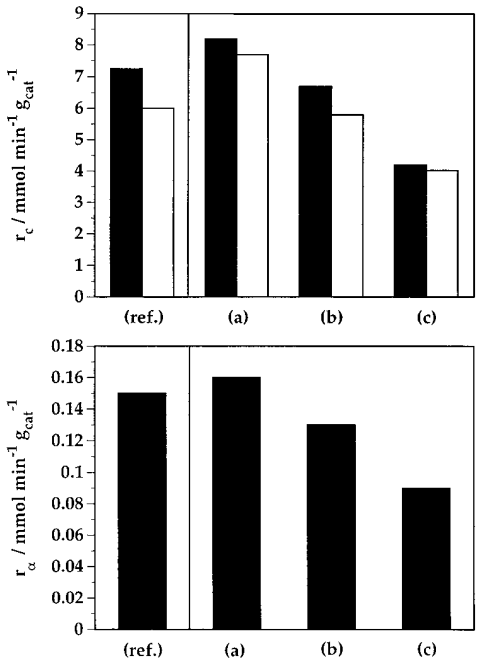

FIG. 7. Initial rates r_c and r_α, defined as epoxide formation in the first 300 s and 20 min, respectively, of *LT* aerogels: (ref.) 10*LT* taken from Ref. (2), (a) 20*LT*720, (b) 30*LT*720, and (c) 50*LT*720. ■, Uncalcined aerogel; □, corresponding samples calcined in air at 673 K. (Top) Epoxidation of cyclohexene (r_c). (Bottom) epoxidation of α-isophorone (r_α). Designations of samples and reaction parameters are explained under Methods.

The steric hindrance is of secondary importance, as shown in part III (3). The uncalcined sample 20*LT*720 exhibited the highest activity ($r_\alpha = 0.17$ mmol min^{-1} g_{cat}^{-1}), whereas 50*LT*720 was least active ($r_\alpha = 0.09$ mmol min^{-1} g_{cat}^{-1}). Again 70*LT*720 exhibited hardly any activity, probably due to its unfavorable textural properties. As reported in part III (3), the calcination of the raw aerogel catalysts led to a decrease in the activity in the epoxidation of cyclohexene and isophorone (by 10–20%).

The initial rates of the epoxidation reaction of cyclohexene (r_c), using the uncalcined 20*LT* series with different aging treatments as catalysts, are represented in Fig. 8. The performance of the uncalcined 20*LT*240 was best ($r_c = 8.5$ mmol min^{-1} g_{cat}^{-1}). In general, the aging time exerted negligible influence on the catalytic activity. The change in the water : alkoxide : acid ratio from 5 : 1 : 0.09 to 5 : 1 : 0.045 distinctly lowered the initial rate of 20*LT*s720 ($r_c = 6.8$ mmol min^{-1} g_{cat}^{-1}). The aerogel 20*LT*ps6.5m, prehydrolyzed and aged for 6.5 months, showed a slight increase in activity ($r_c = 7.1$ mmol min^{-1} g_{cat}^{-1}) compared to aerogel 20*LT*s720, but the activity was still distinctly lower than that of 20*LT*48, 20*LT*240, and 20*LT*720, respectively.

In essence, the uncalcined low-temperature aerogel 20*LT*720 exhibited best catalytic performance in both epoxidation reactions investigated.

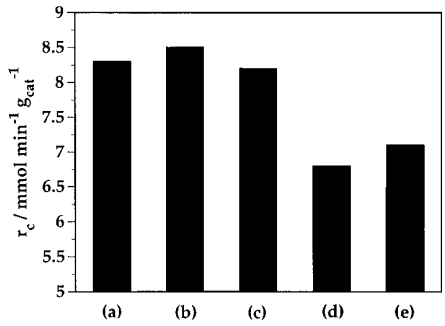

FIG. 8. Initial rate (r_c), defined as cyclohexene oxide formation in the first 300 s, of the 20*LT* series samples: (a) 20*LT*42, (b) 20*LT*240, (c) 20*LT*720, (d) 20*LT*s720, and (e) 20*LT*ps6.5m. All samples were uncalcined.

DISCUSSION

Influence of Ti Content

Favorable textural properties and the highest fraction of Si–O–Ti connectivity ($S_{(Si–O–Ti)}/S_{(Si–O–Si)}$) was achieved by the aerogel 30*LT*720 (Table 2). These properties did, however, not result in a rise in catalytic activity compared to the aerogel 20*LT*720 with lower BET surface area, specific pore volume, pore size maximum, and $S_{(Si–O–Ti)}/S_{(Si–O–Si)}$ value (Table 2). A possible explanation for this behavior is the distinctly lower $D_{(Si–O–Ti)}$ value, indicating lower mixing efficiency and, consequently, the presence of titania nanodomains, which are independently indicated in the UV–Vis spectra by a shift of the absorption edge (Fig. 6). The highest initial rate per mol Ti, representing the catalytic efficiency of the "single" titanium atom, was found for the 10*LT* series (2). Consequently, the continuous decline in mixing efficiency leads to a loss in catalytic activity. These investigations fully agree with the findings in parts I–III (1–3), where only Ti species highly dispersed in the silica matrix were found to be active for the epoxidation reaction.

Influence of Aging Time

The 20*LT* series indicates an influence of the aging time on the textural properties of the low-temperature aerogels (Table 3). The longer the wet sol–gel product was aged, the higher the BET surface areas were. Different authors made similar observations. Scherer (9) showed that chemical reactions leading to gelation continue long after the solution gelled, causing changes in the composition and structure of the gels. Rangarajan and Lira (8) found that aging alcogels in their pore liquor results in reduced drying shrinkage during the extraction procedure with supercritical CO_2. They claim that on aging the processes of dissolution and reprecipitation result in a removal of the microporosity of the wet sol-gel product. Adsorption forces the most likely cause of shrinkage, increase with decreasing

pore size. Consequently, aging of the gel led to less shrinkage, which is in agreement with our results (Table 3).

The aerogel 20*LT*240 showed the highest specific pore volume and best initial rate r_c. In general, however, the aging time had little influence on the catalytic behavior (Fig. 8) although the carbon contents in the 20*LT* series were largely different (Fig. 5). The increase in aging time led to a distinct rise in the amount of residual organic species, that might influence the wetability of the catalysts. Uncalcined low-temperature aerogels are supposed to possess a hydrophobic surface, whereas the calcined samples with C contents in the range 4.5–0.1 wt% should become more hydrophilic with decreasing carbon contents.

Influence of Acid and Prehydrolysis

A change in the molar ratio water : alkoxide : acid let to similar textural properties, carbon contents, and $S_{(Si–O–Ti)}/S_{(Si–O–Si)}$ values, but to lower initial rates r_c. Thus, the amount of acid used in the sol–gel procedure influenced the catalytic activity. Prehydrolysis and aging for 6.5 months hardly affected the initial rates. From part II of this series (2) we know that prehydrolysis of the silicon alkoxide together with chemical modification of the titania precursor had no significant influence on catalytic activity.

CONCLUSIONS

Titania–silica low-temperature aerogels with 20 wt% nominal TiO_2 yield optimum textural properties and Ti dispersion for the use as epoxidation catalysts for bulky reactants. An increase of the Ti loading to 30 wt% nominal TiO_2 leads to a maximum of Si–O–Ti species and larger TiO_2 agglomerates and, consequently, to lower Ti dispersion and minor catalytic activity. Aging of the wet sol–gel product strengthens the gel network, which enhances stability against syneresis during the extraction procedure and thus increases porosity of the dried aerogel. The acid in the hydrolysant, catalyzing the hydrolysis of the alkoxides, influences, the catalytic activity in the investigated epoxidation reaction. Reduction of the acid amount used in the wet sol–gel synthesis lowered the initial rate of the resulting aerogel catalyst. The best catalytic performance for the epoxidation of both cyclohexene and α-isophorone is achieved by a low-temperature aerogel containing 20 wt% TiO_2 and prepared without prehydrolysis using a molar ratio water : alkoxide : acid of 5 : 1 : 0.09 and aging the wet sol–gel state for 240 h.

ACKNOWLEDGMENTS

Financial support of this work by the "Kommission zur Förderung der Wissenschaftlichen Forschung" and F. Hoffmann-La Roche Ltd., Switzerland, is gratefully acknowledged.

REFERENCES

1. Dutoit, D. C. M., Schneider, M., and Baiker, A., *J. Catal.* **153**, 165 (1995).
2. Hutter, R., Mallat, T., and Baiker, A., *J. Catal.* **153**, 177 (1995).
3. Hutter, R., Mallat, T., and Baiker, A., *J. Catal.* **157**, 665 (1995).
4. Brinker, C. J., and Scherer, G. W., "Sol-Gel Science—The Physics and Chemistry of Sol-Gel Processing." Academic Press, San Diego, 1990.
5. Deshpande, R., Hua, D., Smith, D. M., and Brinker, C. J., *J. Noncryst. Solids* **144**, 32 (1992).
6. Davis, P. J., Brinker, C. J., and Smith, D. M., *J. Noncryst. Solids* **142**, 189 (1992).
7. Walther, K. L., Wokaun, A., Handy, B. E., and Baiker, A., *J. Noncryst. Solids* **134**, 47 (1991).
8. Rangarajan, B., and Lira, C. T., *Mater. Res. Soc. Symp. Proc.* **271**, 559 (1992).
9. Scherer, G. W., *J. Noncryst. Solids* **100**, 77 (1988).
10. Livage, J., Henry, M., and Sanchez, C., *Prog. Solid State Chem.* **18**, 259 (1988).
11. Aizawa, M., Nosaka, Y., and Fujii, N., *J. Noncryst. Solids* **128**, 77 (1991).
12. Handy, B. E., Maciejewski, M., Baiker, A., and Wokaun, A., *J. Mater. Chem.* **2**(8), 833 (1992).
13. Miller, J. B., Johnston, S. T., and Ko, E. I., *J. Catal.* **150**, 311 (1994).
14. Barrett, E. P., Joyner, L. G., and Halenda, P. P., *J. Am. Chem. Soc.* **73**, 373 (1951).
15. Harkins, W. D., and Jura, G., *J. Chem. Phys.* **11**, 431 (1943).
16. Sing, K. S. W., Everett, D. H., Haul, R. A. W., Moscou, L., Pierotti, R. A., Rouquérol, J., and Siemieniewska, T., *Pure Appl. Chem.* **57**, 603 (1985).
17. Duran, A., Serna, C., Fornes, V., and Fernandez-Navarro, J. M., *J. Noncryst. Solids* **82**, 69 (1986).
18. Salvado, I. M. M., and Navarro, J. M. F., *J. Noncryst. Solids* **147** & **148**, 256 (1992).
19. Bräutigam, U., Meyer, K., and Bürger, H., *in* "EUROGEL '91" (S. Vilminot, R. Nass and H. Schmidt, Eds.), p. 335. Elsevier, Amsterdam, 1992.
20. Beghi, M., Chiurlo, P., Costa, L., Palladino, M., and Pirini, M. F., *J. Noncryst. Solids* **145**, 175 (1992).
21. Schraml-Marth, M., Walther, K. L., Wokaun, A., Handy, B. E., and Baiker, A., *J. Noncryst. Solids* **143**, 93 (1992).
22. Bertoluzza, A., Fagnano, C., Morelli, M. A., Gottardi, V., and Guglielmi, M., *J. Noncryst. Solids* **48**, 117 (1982).
23. Best, M. F., and Condrate, R. A., *J. Mater. Sci. Lett.* **4**, 994 (1985).
24. Schneider, M., and Baiker, A., *Catal. Rev.-Sci. Eng.* **37**, 515 (1995).